Advanced Ceramics Progress

Research Article

Investigating the Kinetic Parameters of SiO₂-Al₂O₃-CaO-CaF₂-K₂O Oxyfluoride Glass

M. Soleymani Zarabad [a], M. Rezvani [a] *

[a] Department of Materials Science and Engineering, University of Tabriz, Tabriz, East Azerbaijan, Iran

A R T I C L E I N F O

A B S T R A C T

Oxyfluoride glass-ceramics containing CaF_2 nanocrystals are kind of attractive materials for the optical applications due to their low phonon energy and high transparency. Moreover, the crystallization control and consequently, the kinetic properties are important for oxyfluoride glasses. Therefore, in the present research, the crystallization kinetics of isochronal transformation of the $37.26SiO_2$-$28.11Al_2O_3$-$7.73CaO$-$26.89CaF_2$-4.5 K_2O (wt%) glass have been determined upon the basis of maximum transformation rate using Differential Thermal Analysis (DTA) technique. Hence, it is concluded that the crystallization of the mentioned glass is a process controlled by Avrami nucleation, three-dimensional diffusion-controlled growth, and anisotropic growth impingement mode. The effective activation energy Q_p=181 kJ.mol^{-1}, growth exponent n=2.272, nucleation activation energy Q_N= 123, and growth activation energy Q_G=211 have been determined.

1. INTRODUCTION

Rare-earth doped glass-ceramics have been developed for different optical devices such as optical fiber, optical amplifier, infrared, visible laser, and specially night vision cameras [1, 2]. Fluoride glasses and their crystals indicate a high transparency in infrared to the ultraviolet region [3, 4] in addition to the low phonon energy (<500cm^{-1}) [5, 6]. However, they have low chemical and mechanical stability and thus, their preparation is highly limited [7]. Oxyfluoride glass-ceramics were developed to overcome the drawbacks of silicate glasses and fluorides as the hosts of rare-earth ions [8, 9]. Nucleation and growth of fluoride crystals, such as CaF_2, occur in the parent glass matrix during the heat treatment and rare-earth ions preferentially segregate into these fluoride crystals [1]. The crystallization process in amorphous materials provides the interesting aspects of solid states phase transformation. The transformation kinetics model of Johnson-Mehl-Avrami-Kolmogorov (JMAK) describes the transformation of a material into another phase during an isochronal or isothermal phase

transformation as a function of temperature and time, respectively, which can be used when the JMA model cannot be used [10]. This model was modified to Liu-Sommer-Mittemeijer (LSM). The evaluation of the maximum transformation rate was used for isochronal and isothermal transformations including different modes of nucleation, growth, and impingement. This method has been applied to determine the impingement mode and consequently, the activation energies for nucleation and growth separately. This method has been used successfully on the Mg–Cu–Y metallic glass crystallization [11].

In this research, the Aluminosilicate based oxyfluoride glasses with $37.26SiO_2$-$28.11Al_2O_3$-$7.73CaO$-$26.89CaF_2$ (wt%) composition were prepared through the conventional melt-quenching method. This composition was selected since the aluminosilicate based glass can provide necessary optical transparency and strength for optical applications. In addition, the glass can maintain transparency after the heat treatment for crystallization of fluoride nanocrystals [7, 8]. The non- isothermal kinetics analysis known as LSM (Liu-Sommer-Mittemeijer)

* Corresponding Author Email: m_rezvani@tabrizu.ac.ir (M. Rezvani)

based on maximum transformation rate [12, 13] was applied for the oxyfluoride glasses to investigate the crystallization kinetic and to determine the impingement mode, growth exponent, and separate activation energies of nucleation and growth.

2. EXPERIMENTAL PROCEDURE

$37.26SiO_2$-$28.11Al_2O_3$-$7.73CaO$-$26.89CaF_2$-$4.5K_2O$ (wt %) glasses were prepared using precursor powders. The mentioned composition is the most typical one for the basic glass, which has also been used by other scientists [14- 18]. The main starting materials are high purity leached SiO_2 (99% purity), Al_2O_3 (Merck 101077), and CaF_2 (Dae Jung 2508145). $CaCO_3$ (Merck 102069) and K_2CO_3 (Sigma-Aldrich P5833) were applied to introduce CaO and K_2O. To avoid bubbles in the samples, Sb_2O_3 and As_2O_3 were used as refining agents. K_2O was added to the batch to have a melt with favorable viscosity [18]. 50g of the batch was mixed and poured in alumina crucibles, heated with the rate of $10°C.min^{-1}$, and finally melted at 1723K (1450°C) for 1 hour in an electric furnace.

Then melt was poured into the preheated stainless steel molds, which were heated at 773K (500°C) and used to shape the molten glass, then were cooled in air. Finally, obtained glassy discs with a thickness as much as 0.5cm were annealed at 773K (500°C) for 30 min to release the internal stresses arose from thermal shock.

The crystal phase analysis of glass-ceramics was carried out by X-Ray diffraction (XRD, Siemens D-500). In this research, the X-ray diffraction just used to ensure that there is not any crystallization during the cooling procedure of the melt and to determine the crystal structure of the crystallized phase after heat treatment.

The differential thermal analysis (DTG- 60AH Shimadzu) of powdered glass samples was carried out through different heating rates of 5, 10, 15 and $20°C.min^{-1}$ to determine the crystallization temperatures. About 50mg of powdered glass was analyzed by differential thermal analysis (DTA) for Kinetic calculations to investigate the crystallization behavior.

The sample preparation for scanning electron microscopy (SEM) included polishing, etching in a 5% HF solution for 30 seconds and finally applying gold-coat. Subsequently, the SEM observations of the prepared sample were carried out through Tescan MIRA3 FEG- SEM.

3. RESULTS AND DISCUSSION

The composition of glass $37.26SiO_2$-$28.11Al_2O_3$-$7.73CaO$-$26.89CaF_2$-$4.5K_2O$ (wt %) is shown in Table 1.

TABLE 1. Composition of the glass $37.26SiO_2$-$28.11Al_2O_3$-$7.73CaO$-$26.89CaF_2$-$4.5K_2O$

Composition (wt %)						
SiO_2	Al_2O_3	CaO	CaF_2	K_2O	As_2O_5	Sb_2O_5
37.26	28.11	7.73	26.89	4.5	0.2	0.2

The melted oxyfluoride glass was heat-treated at about Tp (based on DTA results) to determine the crystalline phase. Figure 1 (a) and (b) show the image of oxyfluoride glass and XRD patterns of the as-prepared and the heat-treated glasses at 952K for 1h, respectively. The amorphous structure of as-prepared sample and the crystalline peaks of the heat-treated sample (indexed as CaF_2 crystals) are illustrated in Figure 1 (b).
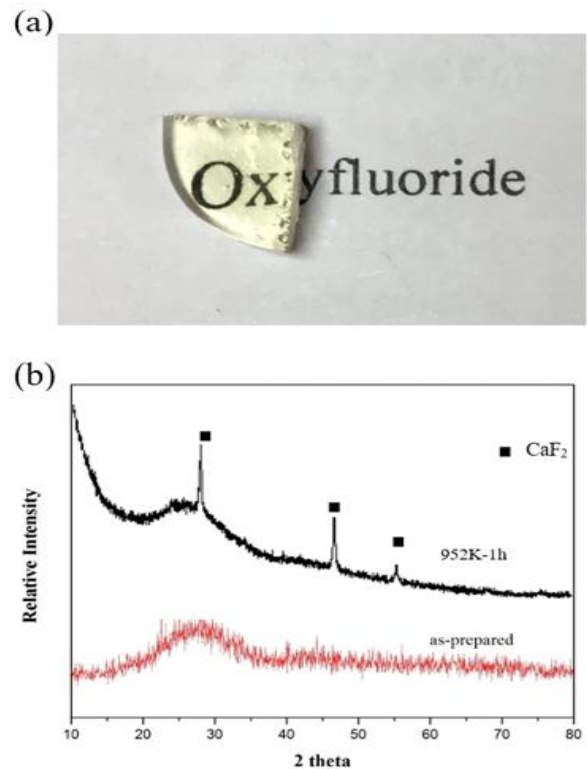

Figure 1. (a) Photograph of as-prepared oxyfluoride glass and (b) XRD patterns of oxyfluoride glass and glass-ceramic which are heat-treated at 952K (T_{p1}) for 1h

About 20mg powder samples were poured in a standard platinum crucible and scanned in room temperature to complete crystallization at different heating rates from 5 to 20 $K.min^{-1}$. DTA curves were studied for determination of the crystallization temperature and studying of kinetic properties. Figure 2 shows a series of DTA curves measured at different heating rates (Φ) of 5,

10, 15, and 20 K.min^{-1}. Table 2 illustrates the summarized information of Figure 2 including the glass transition temperature (T_g), the onset temperature of the first phase crystallization (T_{ost}), the maximum crystallization temperature of the first phase (T_{p1}), and the crystallization temperature of the second phase (T_{p2}). The first peak is attributed to the crystallization of CaF_2 at the heating rate of 10K min^{-1} and temperature about 952K and the second one is related to the crystallization of $Ca_2Al_3O_6F$ at a temperature about 1179K [19].
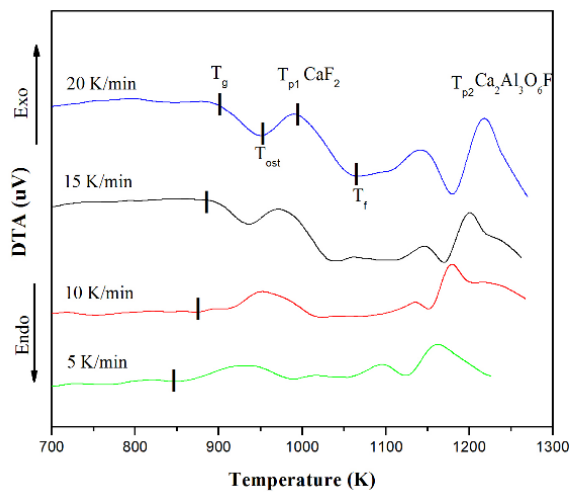

Figure 2. DTA curves of the oxyfluoride glass measured at different heating rates

According to the DTA results, all of the above characteristic temperatures increase by increasing the heating rate (Φ), which illustrate that the crystallization of these two phases is a kinetic process. , The kinetic properties of CaF_2 phase will be studied due to its optical importance. The crystallization fraction f is f= (AT/A) at a given temperature of T. Where A is the total area of the exothermic peak between Tost (where the crystallization begins) and Tf (where the crystallization completes) and AT is the area between Tost and desired temperature T.

TABLE 2. Characteristic temperatures values of the glass at different heating rates

Φ (K min^{-1})	T_g /K	T_{ost}/K	T_{p1}/K	T_{p2}/K
5	843	870	932	1161
10	874	911	952	1179
15	884	932	971	1200
20	899	962	990	1218

The transformed fraction, which does not overlap the new phase particles is given in the form of equation (1) [12].

$$X_e = (k\alpha)^n = \left(K_0 \alpha exp \left(-\frac{Q}{RT} \right) \right)^n \qquad (1)$$

Where α represents RT^2/Φ for isochronal transformation's and K_0 is the rate constant and the pre-exponent factor of the rate constant, respectively. Q stands for the effective activation energy and n shows the growth or Avrami exponent. T, t, R, and Φ are the temperature, time, gas constant, and constant heating rate, respectively. In this model, the impingement mode would result in the real transformed fraction (f). The transformation degree (f) is related to the extended transformation degree (X_e) by impingement modes (random nuclei dispersion, anisotropic growth, non-random nuclei).

The evolution of df/dT versus T (Figure 3(a)) was carried out using f versus T (Figure 3(b)) and the df/dT versus f (Figure 3(c)) for the crystallization of 37.26SiO$_2$-28.11Al$_2$O$_3$-7.73CaO-26.89CaF$_2$-4.5K$_2$O (wt %) oxyfluoride glass system. The f_p (a quantity for f at maximum transformation rate) values were obtained from the graphs and listed in Table 3.

TABLE 3. The values of f_p, and n_p

Φ/K min^{-1} ($^{\circ}$C min^{-1})	T_p	f_p	ξ	n_p
5	932	0.6131	1.1086	2.105
10	952	0.6040	1.1632	2.236
15	971	0.5778	1.3342	2.332
20	990	0.5585	1.4772	2.416

It has been found out that f_p values are less than 0.632 for all different transformations rates, which means that prevailing impingement mode is due to the anisotropic growth According to the impingement mode equations, which are mentioned above, the position of transformation rate maximum (f_p) will increase in the case of "non-random nuclei dispersion" with increasing ε and the position of transformation rate maximum (f_p) will decrease in case the of "anisotropic growth impingement" with increasing ξ [11]. So from the position of f_p, the values of ξ and ε (impingement factors) can be determined.
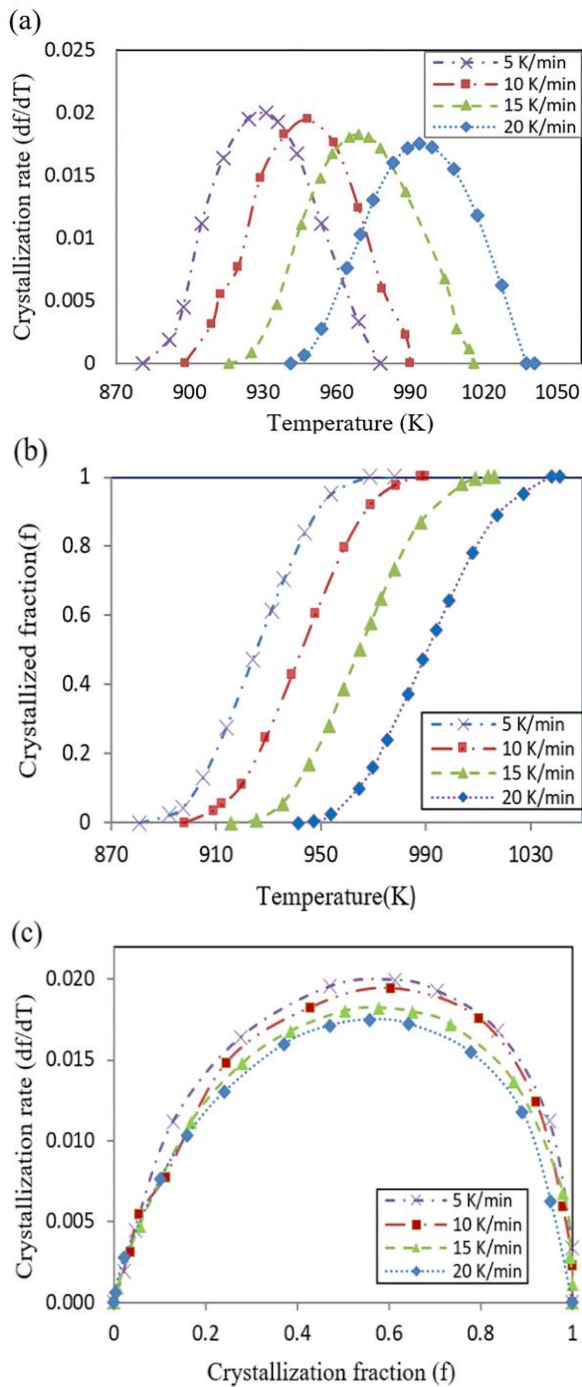
(a)

(b)

(c)

Figure 3. Evolution of: (a) df/dT versus T, (b) f versus T and (c)df/dT versus f for isochronal transformation of 37.26SiO$_2$-28.11Al$_2$O$_3$-7.73CaO-26.89CaF$_2$-4.5K$_2$O glass system (Φ=5, 10, 15 and 20 (℃/min))

As shown in Figure 4, anisotropic growth impingement is prevailing at 37.26SiO$_2$-28.11Al$_2$O$_3$-7.73CaO-26.89CaF$_2$-4.5K$_2$O glass system with the decreasing values of fp with increasing the ξ. Moreover, Figure 5 shows the cross-sectional SEM image of the glass

system, which is heat-treated for 1h at Tp. The values of ξ for different heating rates are listed in Table 3.
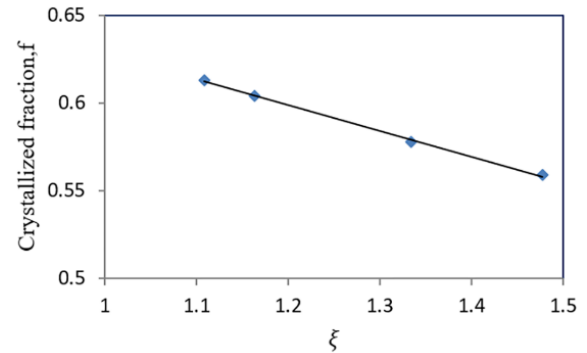

Figure 4. Evolution of f versus ξ for 37.26SiO$_2$-28.11Al$_2$O$_3$-7.73CaO-26.89CaF$_2$-4.5K$_2$O glass system

Further kinetic information can be obtained using maximum transformation rate analyzing after determination of the impingement mode. With regard to isochronal analysis, the np value is obtained from the equation (2).

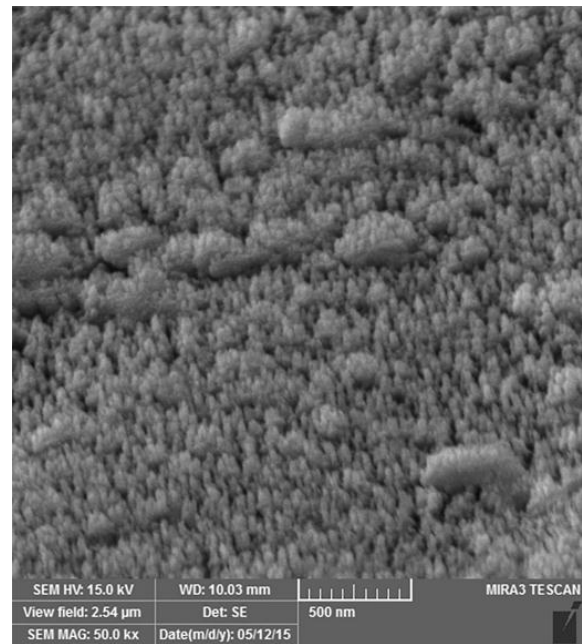$$n_p = \frac{RT_p^2}{Q_p + 2RT_p}\left(\frac{d\, lnX_e}{dT}\right)_p \qquad (2)$$

Figure 5. Cross-sectional SEM image of 37.26SiO$_2$-28.11Al$_2$O$_3$-7.73CaO-26.89CaF$_2$-4.5K$_2$O glass-ceramic

Although the expression of Xe follows from the identified different impingement mode in Equations (2)-(5) in isochronal transformations, the quantity of Q_p is necessary to determine the np value. The value of Q_p can be determined using a Kissinger-like analysis as equation (3) [12, 13].

$$\frac{d\left(ln\frac{RT_p^2}{\Phi}\right)}{d\left(\frac{1}{T_p}\right)} = \frac{Q_p}{R} \qquad (3)$$

As it is shown in Figure 6, Q_p is calculated around 181 kJ.mol^{-1} from the slope of the $ln\frac{RT_p^2}{\Phi}$ versus $\frac{1}{T_p}$ plot by applying Equation 10 to the data in Figure 6. After np, the growth exponent was obtained using Equation 9 and the data were listed in table 3. The isochronal annealing results in Refs. [11, 12, 20] show an increase in np along with increasing the Φ, which is compatible with Avrami nucleation. The data in Table 3 show that np increases with increasing the Φ in this oxyfluoride glass system. Crystallization mechanism of CaF$_2$ in oxyfluoride glasses is a three-dimensional, volume diffusion-controlled growth process [20].
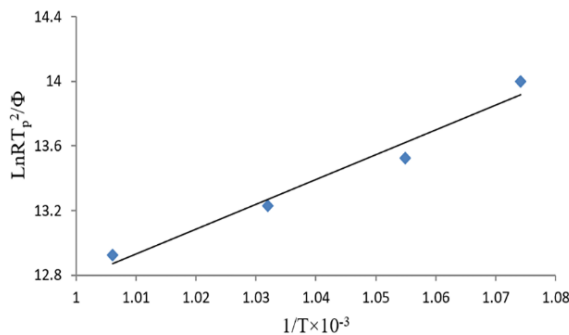

Figure 6. Determination of effective activation energy from the data in Figure 3

According to volume diffusion-controlled growth theory, the Avrami exponent is described as equation (4) [21].

$$n = a + bm \qquad (4)$$

Where a is nucleation index (a=0 when nucleation is zero, a>1 for the increasing nucleation rate, 0<a<1 when the nucleation rate is decreasing, and a=1 for the constant nucleation rate), b is the dimensionality of growth (b=1,

2, or 3 for one-dimensional, two-dimensional, or three-dimensional growth respectively), and m is growth index (m=0.5 is for diffusion-controlled growth mode and m=1 is for interface controlled growth mode). In the Avrami exponent, n for this oxyfluoride system varies from 2.10 to 2.42. The average Avrami exponent about 2.272 gives b=3, m=0.5, and 0<a<1, which implies the main diffusion-controlled three-dimensional growth with an Avrami decreasing nucleation rate during the crystallization. As shown in Table 3, the value of n for the oxyfluoride amorphous glass increases with increasing the heating rate. According to the DTA curves in Figure 2, it is clear that the transformation temperature increases with increasing the heating rate. Therefore, the values of n increase with increasing transformation temperature because the atomic diffusion is difficult at low temperatures, which results in retardation of nucleation and growth process and leads to a lower nucleation rate. At higher transformation temperatures, the diffusion of atoms will be relatively easy, which will increase the nucleation rate. It means that the nucleation and growth rates are not constant during the crystallization process.

The value of effective activation energy Q_p, which is obtained using Equation 10 and the maximum transformation rate data from Figure 3 is about 181 kJ.mol^{-1}.

As mentioned before, an equation can be used to determine the activation energy of nucleation Q_N with consideration the Avrami nucleation for this oxyfluoride system [10] as equation (5).

$$ln\left(\frac{\alpha}{\frac{1}{n_p-d/m}-1}\right) = -\ln A + Q_N/R\,T_P \qquad (5)$$

plotting $ln\left(\frac{\alpha}{\frac{1}{n_p-d/m}-1}\right)$ vs $1/Tp$. Where α is identified as RT^2/Φ for isochronal transformations and m is the growth mode parameter, which is equal to 2 for volume diffusion-controlled growth and d is the dimensionality of growth, which is equal to 3 in this system. It is concluded that d/m=3/2, so Q_N=123 kJ.mol^{-1} is obtained.

Then Q_G follows from equation (6) [12].

$$Q_G = \frac{n_p(Q_p - Q_n)}{d/m} + Q_N \qquad (6)$$

According to the obtained results for Q_p and np and using equation 6, the Q_G value is obtained as much as 211 kJ.mol^{-1}.

The characteristic parameters of the process are determined through fitting the numerical description of

the transformation basis with experimental data in principle, which are physically significant [10]. From the above obtained kinetic information of $37.26SiO_2$-$28.11Al_2O_3$-$7.73CaO$-$26.89CaF_2$-$4.5K_2O$ glass system, it is argued that the crystallization of mentioned system is governed by Avrami nucleation, three-dimensional diffusion-controlled growth, and anisotropic growth impingement mode. Accordingly, a new equation will be obtained considering Equation 1 and fraction transformed during impingement due to anisotropic growth.

$$f = 1 - \left\{ 1 + (\xi - 1)\left[k_0{}^n \left(\frac{RT^2}{\Phi} \right)^n exp\left(-\frac{nQ}{RT} \right) \right] \right\}^{\frac{-1}{\xi-1}} \quad (7)$$

Consequently, the exact kinetic data was obtained by fitting the resulting equation (equation 7) with experimental data of f versus T and df/dT versus T (Figure 3a and Figure 3b). The obtained kinetic data of $K_0{}^n$, n, Q are shown in Table 4. The resulted values of n and Q are compatible with obtained experimental data from analysis of maximum transformation rate. This also proves that the isochronal crystallization mechanism of $37.26SiO_2$-$28.11Al_2O_3$-$7.73CaO$-$26.89CaF_2$-$4.5K_2O$ glass is based on Avrami nucleation, three-dimensional diffusion-controlled growth, and anisotropic growth impingement mode

TABLE 4. Model parameters determined by fitting the curve of *f* versus *T* and df/dT versus T for the $37.26SiO_2$-$28.11Al_2O_3$-$7.73CaO$-$26.89CaF_2$-$4.5K_2O$ glass system, which was crystallized by the mechanism of Avrami nucleation, three-dimensional diffusion-controlled growth, and anisotropic growth impingement mode

Parameter	$K_0{}^n$	n	Q (kJ.mol^{-1})	Error%
Value	3.77E+10	2.457	183.44	0.65

4. CONCLUSION

According to the analytical phase transformation model, the kinetic data of the isochronal crystallization of $37.26SiO_2$-$28.11Al_2O_3$-$7.73CaO$-$26.89CaF_2$-$4.5K_2O$ (wt %) glass have been determined. The crystallization of the mentioned glass is a process controlled by Avrami nucleation, three-dimensional diffusion-controlled growth, and anisotropic growth impingement mode. The effective activation energy, growth exponent, nucleation activation energy, and growth activation energy have been determined as much as Q_P=181 kJ.mole^{-1}, n=2.272, Q_N= 123, Q_G=211, respectively.

REFERENCES

1. Lavín, V., Lahoz, F., Martín, I. R., Rodríguez-Mendoza, U. R., "Optical properties of rare-earth ions in transparent oxyfluoride glass-ceramics", In Balda, R., ed., *Photonic Glasses, Research Signpost,* Kerala, India, (2006), 115-149. https://www.academia.edu/download/46573097/54-Photonic_Glasses_Chapter_6.pdf

2. Upadhyaya, G. S., "*Holland, W., Beall, G.: Glass-Ceramic Technology, "The American Ceramic Society", Westerville, OH, USA, 2002, pp. 372*", *Science of Sintering*, Vol. 36, No. 3, (2004), 215-216. https://doi.org/10.2298/sos0403216u

3. Gonçalves, C. M., Santos, L. F., Almeida, R. M., "Rare-earth-doped transparent glassceramics", *Comptes Rendus Chimie*, Vol.5, No. 12, (2002), 845–854. https://doi.org/10.1016/S1631-0748(02)01457-1

4. Farahinia, L., Rezvani, M., "Luminescence Properties of Oxyfluoride Glass and Glass-ceramic Doped with Y^{3+} Ions", *Advanced Ceramics Progress*, vol. 1, No. 1, (2015), 6-10. https://dx.doi.org/10.30501/acp.2015.70000

5. Adam, J, L., "Non-oxide glasses and their application in optics", *Journal of Non-Crystalline Solids*, Vol. 287, No. 1-3, (2001), 401–404. https://doi.org/10.1016/S0022-3093(01)00632-9

6. Adam, J. L., "Lanthanides in Non-Oxide Glasses", *Chemical Reviews*, Vol. 102, No. 6, (2002), 2461–2476. https://doi.org/10.1021/cr010305b

7. Dejneka, M. J, "Transparent oxyfluoride glass ceramics", *Materials Research Society Bulltin*, Vol. 23, No. 11, (1998), 57–62. https://doi.org/10.1557/s0883769400031018

8. Qiao, X., Fan, X., Wang, M., "Luminescence behavior of Er^{3+} in glass ceramics containing BaF_2 nanocrystals", *Scripta Materialia*", Vol. 55, No. 3, (2006), 211-214. https://doi.org/10.1016/j.scriptamat.2006.04.023

9. Ye, S., Zhu, B., Chen, J., Luo, J., Qiu, J. R., "Infrared quantum cutting in Tb^{3+}, Yb^{3+} co-doped transparent glass ceramics containing CaF_2 nanocrystals", *Appllied Physics Letters*, Vol. 92, No. 14, (2008), 141112. https://doi.org/10.1063/1.2907496

10. Moharram, A. H., Abdel-Baset, A. M., Shokr, F. S., "Crystallization kinetics of the $Se_{80}Te_{15}Sb_5$ glass", *Chalcogenide Letters*, Vol. 13, No. 9, (2016), 435–442. http://chalcogen.ro/435_MoharramAH.pdf

11. Liu, F., Song, S. J., Sommer, F., Mittemeijer, E. J., "Evaluation of the maximum transformation rate for analyzing solid-state phase transformation kinetics", *Acta Materialia*, Vol. 57, No. 20, (2009), 6176–6190. https://doi.org/10.1016/j.actamat.2009.08.046

12. Liu, F., Sommer, F., Bos, C., Mittemeijer, E. J., "Analysis of Solid State Phase Transformation Kinetics: Model and Recipes", *International Materials Reviews*, Vol. 52, No. 4, (2007), 193-212. https://doi.org/10.1179/174328007X160308

13. Mittemeijer. E. J., "Analysis of the kinetics of phase transformations", *Journal of Materials Science*, Vol. 27, No. 15, (1992) 3977-3987. https://doi.org/10.1007/bf01105093

14. Kishi, Y., Tanabe, S., "Infrared-to-visible up-conversion of rare-earth doped glass ceramics containing CaF_2 crystals", *Journal of Alloys and Compounds*, Vol. 408, (2006), 842-844. https://doi.org/10.1016/j.jallcom.2005.01.096

15. Babu, P., Jang, K. H., Kim, E. S, Shi, L., Seo, H. J., "Optical Properties and White-Light Emission in Dy^{3+}-Doped Transparent

Oxy-fluoride Glass and Glass Ceramics Containing CaF$_2$ Nanocrystals", ***Journal of the Korean Physical Society***, Vol. 54, No. 4, (2009), 1488-1491. https://doi.org/10.3938/jkps.54.1488

16. Sun, X. Y., Gu, M., Huang. S. M, Jin, X. J., Liu, X. L., Liu, B., Ni, C., "Luminescence behavior of Tb^{3+} ions in transparent glass and glass-ceramics containing CaF$_2$ nanocrystals", ***Journal of Luminescence***, Vol. 129, No. 8, (2009), 773-777. https://doi.org/10.1016/j.jlumin.2009.02.017

17. Sun, X. Y. and Huang. S. M., "Tb^{3+}-activated SiO$_2$–Al$_2$O$_3$–CaO–CaF$_2$ oxyfluoride scintillating glass ceramics", ***Nuclear Instruments and Methods in Physics Research Section A: Accelerators, Spectrometers, Detectors and Associated Equipment***, Vol. 621, No 1-3, (2010), 322-325. https://doi.org/10.1016/j.nima.2010.04.032

18. Farahinia, L., Rezvani, M., "Optical property evaluation of oxy-fluoride glasses doped with different amounts of Y^{3+} ions",

Journal of Non-crystalline Solids, Vol. 425, (2015), 158-182. https://doi.org/10.1016/j.jnoncrysol.2015.03.014

19. Imanieh, M. H., EftekhariYekta, B., Marghussian, V., Shakhesi, S., Martín, I. R., "Crystallization of nano calcium fluoride in CaF$_2$–Al$_2$O$_3$–SiO$_2$", ***Solid State Sciences***, Vol. 17, (2013) 76–82. https://doi.org/10.1016/j.solidstatesciences.2012.11.008

20. Liu, F., Sommer. F., Mittemeijer, E. J., "Analysis of the kinetics of phase transformations; roles of nucleation index and temperature dependent site saturation and recipes for the extraction of kinetic parameters", ***Journal of Materials Science***, Vol. 42, No. 2, (2007), 573-587. https://doi.org/10.1007/s10853-006-0802-4

21. Ouyang, Y., Wang, L., Chen, H., Cheng, X., Zhong, X., Feng, Y., "The formation and crystallization of amorphous Al$_{65}$Fe$_{20}$Zr$_{15}$", ***Journal of Non-Crystalline Solids***, Vol. 354, No.52-54, (2008), 5555-5558. https://doi.org/10.1016/j.jnoncrysol.2007.02.099